

BEAM DETECTION USING RESIDUAL GAS IONIZATION*

William H. DeLuca
Argonne National Laboratory
Argonne, Illinois

Summary

The nondestructive beam detector systems originated at Argonne National Laboratory allow continuous measurement of the proton beam position and beam profile in the Zero Gradient Synchrotron (ZGS) during the accelerating and targeting cycle. Nondestructive detection is accomplished by collecting the ions produced by the proton beam ionizing residual gas in the vacuum chamber. The amplitude of the electrical currents obtained by collecting these ions onto a variety of electrodes depends on the distribution of the protons in the beam. The characteristics of the electric signals make them suitable as inputs to computer systems. Both analog and digital techniques have been used to determine beam position and profile. These beam detection systems have been used for measuring the properties of the 50 MeV beam between the injector linac and the synchrotron ring; for studying the steering and the radial growth of the size of the beam during acceleration; and for measurements during the targeting sequences.

Introduction

Considerable interest has developed in non-destructive beam profile monitors for high energy particle accelerators. The obvious values of such monitors are continuous on-line measurement of the beam position and profile during acceleration for synchrotron resonance and damping studies.

The need for such monitors at the ZGS arose when accelerated beam intensities exceeded $1(10)^{12}$ protons per pulse. These intensities led to instabilities during acceleration which resulted in beam losses and/or growths. At the time, beam width measurements involved intercepting part of the beam in some fashion. Such methods were limited in value since dynamic measurements were virtually impossible.

A nondestructive profile monitoring system was thus developed and installed in the ZGS in 1967.¹ Since that time a similar system has been installed in the 50 MeV proton line.² Beam detection, in these systems, is accomplished by

the rapid collection of ions generated by proton beam ionization of residual gas (1×10^{-6} torr) in the vacuum chamber. These liberated ions constitute a convenient signal bearing beam distribution information, since at a given energy and pressure, the number of ion pairs produced in a given volume is proportional to the number of protons in that volume.

Assembled in this paper is a description of the systems and their principles of operation, along with some of the results and observations obtained.

Ionization

There are volumes of literature available which analyze in detail the process of ionization by high energy particles.³⁻⁴ However, the published experimental data on ionization only covers an energy range up to several MeV. The following discussion is intended to provide only that information which is of interest when utilizing this phenomenon as a means to detect protons in high energy accelerators.

A charged particle moving through a gas media loses energy due to the excitation and ionization of the gas atoms by inelastic collisions. The loss of energy per centimeter of path is generally referred to as the ionization loss. The electrons ejected in the ionization process may have energies up to several tens of electron volts. Since the ionization potential of various gases is in the order of 20 eV, the electrons are able, at atmospheric pressures, to produce several ion pairs before coming to rest. However, at particle accelerator vacuum chamber pressures where the mean free path between gas molecules is in the tens of meters, secondary ionization is negligible. The average energy required to form an ion pair is commonly found by measuring the total ionization, primary and secondary, caused by a particle of known energy. It is clear that these values are not applicable at low pressures.

F. Rieke and W. Prepejchal⁵ have experimentally measured the specific primary ionization in gases by high energy electrons. Specific primary ionization, S , refers to the number of primary ionization acts per unit path under standard conditions. S can be related to the atomic properties of the vacuum chamber residual gas by means of the Bethe theory.⁶

*Work performed under the auspices of the U. S. Atomic Energy Commission.

Using atomic values for air, obtained by Rieke, S was calculated over an incident proton energy range of 20 MeV to 100 GeV, assuming an air pressure of $1(10)^{-6}$ torr. The calculated values for S are shown in Fig. 1. Also shown in Fig. 1 are the values of S , normalized to $1(10)^{-6}$ torr, measured in the ZGS. As can be seen, there is a very good correlation between the expected and measured values. The difference may be attributed to the uncertainty of the composition of the residual gas and the pressure readings available in the ZGS straight section boxes.

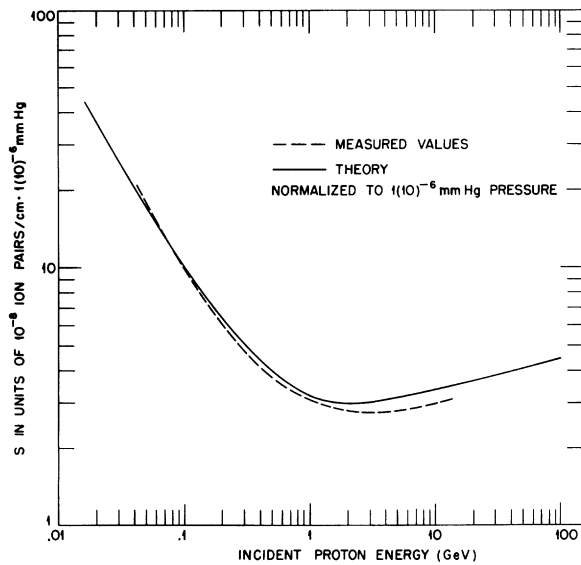


Fig. 1 Comparison of theoretical and measured values of ion pair production as a function of proton energy.

At a vacuum chamber pressure of $1(10)^{-6}$ torr, there exist approximately $3.2(10)^{10}$ gas molecules per cubic centimeter. Utilizing the S curve, one finds that a circulating beam current of 300 mA, corresponding to approximately $1(10)^{12}$ protons at 12 GeV in the ZGS, will liberate $6.5(10)^{10}$ ionpairs per sec (≈ 10.4 nA) per centimeter length of proton beam in a gas pressure of $1(10)^{-6}$ torr. This ion signal is of sufficient amplitude to detect the beam profile distribution.

R. Sternheimer⁷ has calculated the ionization loss, dE/dx , for protons in air with a range of energies from 2 MeV to 100 GeV. At a pressure of $1(10)^{-6}$ torr, his results give the average energy loss per centimeter length of proton travel. Relating Sternheimer's energy loss data and the measured ion pair production, one can conclude that approximately 95 eV is the average energy required to create a primary ion pair by protons in air.

The process of ionization by high energy protons can be analyzed mainly as an interaction between the proton and the orbiting electrons of the residual gas atom. The atom, during the ionization process, remains relatively undisturbed, maintaining a kinetic energy of just a few hundredths of an electron volt. However, once the atom becomes a positively charged ion, a coulomb force interaction with the proton beam results. This interaction tends to scatter the ions. To minimize the scattering, which would result in an erroneous detected beam profile, the ion must be quickly removed from the vicinity of the beam. This phenomenon is illustrated later in this paper.

The liberated electrons receive essentially all the energy in the generation of the ion pair. M. E. Rudd, et al,⁸ has measured the energy and angular distribution of the ejected electrons from helium and hydrogen by proton ionization at various energies up to 0.3 MeV. The ejected electrons have an energy distribution which extends into the tens and hundreds of electron volts; however, the most probable energy is only a few eV. The higher the energy of the liberated electron, the smaller the scattering angle with respect to the path of the incident proton. The coulomb forces acting on the liberated electrons have little effect on those electrons scattered at higher energies. Those electrons scattered at low energies will be attracted to the passing proton beam. Results observed using electron collection are discussed in the next section.

When a beam of positive ions or electrons is incident on a solid surface, a variety of phenomena may result.³ In the first place, secondary electron emission will occur largely in the backward direction from the target surface. The amount of secondary electron emission is dependent on the energy and nature of the incident ion, the angle of impact, and the nature of the target surface. Surface electron secondary emission may be used to enhance the detected ion or electron signal. The secondary emission ratio of certain metals when bombarded by incident ions with a few keV of energy, may be as much as 8. The impact of positive ions on a solid surface also gives rise to sputtering. Atoms or clusters of atoms, are ejected from the surface as a result of impact. These sputtered particles usually move slowly and are sometimes electrically charged. Low energy positive ions striking a solid surface may simply be scattered back with loss of energy. On the other hand, when the ion energy is greater than the surface work function, most of the ions will be neutralized at the surface, and the reflected fraction of incident ions is small.

Detection

A variety of electrode designs utilizing electric and magnetic fields may be employed to collect the ions or electrons generated by the proton beam. To the user, a particular design may prove to be more advantageous for time or spatial resolution, data processing, or display. For example, Johnson and Thorndahl⁹ in the CERN proton synchrotron have successfully used a crossed rotating electric and magnetic fields system of electron collection to scan through the proton beam. The output is processed electronically to provide a visual display.

The systems at the ZGS were designed for simplicity, compatibility as data inputs for the control computer, and a useful operational display, while still achieving good time and spatial resolution. In early 1967, Fred Hornstra¹ constructed the first operational system, Fig. 2a, called the "beam viewer." The liberated electrons are accelerated to several keV to a phosphor screen. Light emitted by the phosphor gives a nondestructive visual measure of the proton beam position and width. The screen is observed with a television camera whose monitor unit is in the Main Control Room. This system has proven invaluable for assisting machine operating personnel during tuneup and targeting at the ZGS.

The second electrode, Fig. 2b, which is being used to obtain ionization and beam profile data, is installed in the synchrotron and in the 50 MeV beam line. The vertical profile electrodes are similar to that of Fig. 2b but aligned for horizontal collection. These electrodes employ a strip electrode detector. An electric field, transverse to the beam direction, exists in the region between the ground screen and the high voltage screen. The ions liberated by the proton beam are accelerated through the ground screen, which provides electrostatic noise shielding, and collected on the strip electrode. A negatively charged secondary screen is used to return secondary electrons to the strip electrode. The ion current collected by each segment of the strip electrode is proportional to the instantaneous beam current in its corresponding section of the vacuum chamber. A simultaneous or rapid sampling of the ion current detected by each of the segments provides a one dimensional incremental beam density profile. The strip electrodes are divided into ten strips. For detecting the synchrotron beam, which is approximately 12 cm wide and 5 cm high, the individual radial electrode strips are 3.8 cm wide and 5.1 cm long and the vertical electrode strips are 1.3 cm high and 10 cm long. For detecting the 50 MeV beam,

which is approximately 2.5 cm in diameter, the individual strips are 5 mm wide and 2.5 cm long on both the horizontal and vertical electrodes.

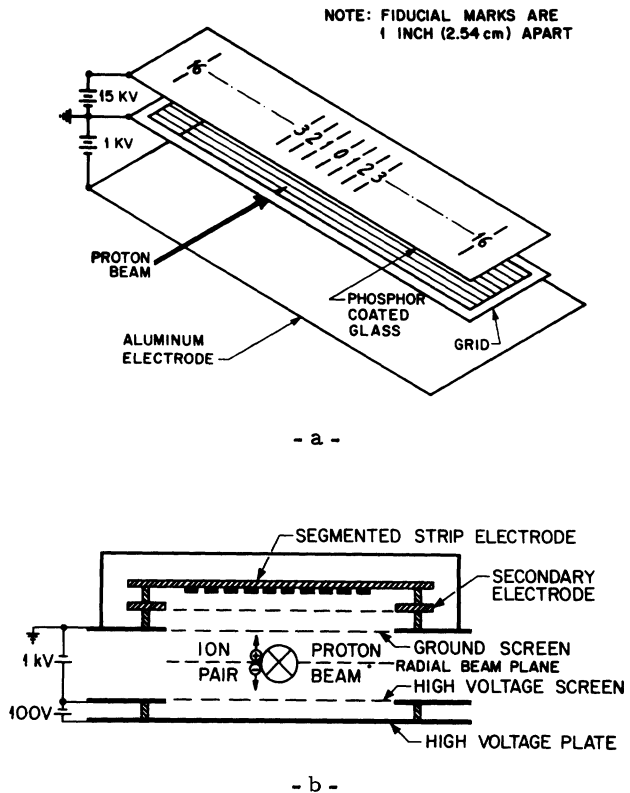


Fig. 2 Nondestructive detection electrodes:
a) synchrotron beam viewer, b) synchrotron strip electrode.

To collect the liberated electrons, the high voltage polarity is reversed from that shown in Fig. 2b. On the synchrotron detector, a screen is included adjacent to the high voltage plate. This screen, when negatively charged, will repel the ion generated secondary electrons back to the high voltage plate. This permits the collection, on the strip electrode, of only those electrons liberated by the proton beam.

Secondary electron emission has been used to amplify the detected signal current. When utilizing ion collection, since the number of secondaries is a function of primary energy, a post accelerating field is required to minimize the energy distribution of the ions striking the detector. In the main ring, an electrode was modified to post accelerate the ions to an energy of 19 keV. This acted as a preamplifier stage and increased the detected ion current signal by approximately a factor of four (the ions were being collected on copper strips).

Secondary electrons created by the ions striking the high voltage plate may be used to enhance the available electron current signal. To intensify the visual image of the beam viewer, the ions are post accelerated to many keV and strike an aluminum high voltage plate. The resulting secondaries are accelerated back to the phosphor screen to brighten the initial electron image. This additional signal increased the sensitivity of the beam viewer considerably.

To provide a true representation of the beam profile, the ions must be transported to the pickup electrode without significant drift transverse to the electric field. Scattering due to the kinetic energy of the ion was measured in the 50 MeV beam line. Two slits were used to collimate the beam to a known size (smaller than one strip width) at the detector location. Moving one of the slits to position the beam successively at the edges of a single segment yields a measure of detected beam width. The difference between the detected and collimated beam widths is a measure of the scattering of the detected ions. The results showed a scattering of $\pm 1/3$ mm using an electric field of 260 V/cm and a collection path length of 5 cm. This corresponds to an ion kinetic energy of 0.014 eV, which is approximately the most probable energy of gas molecules at room temperature assuming a Maxwell-Boltzman energy distribution.

It was also observed that the width of the detected beam profile varied with electric field strength up to a point. Figure 3 illustrates the ion collection path due to its coulomb force interaction with the beam. Consider the 50 MeV proton beam as having a circular cross section with a uniform distribution of protons. It is convenient to express the beam as a line of charge to determine the scattering of the ions generated at

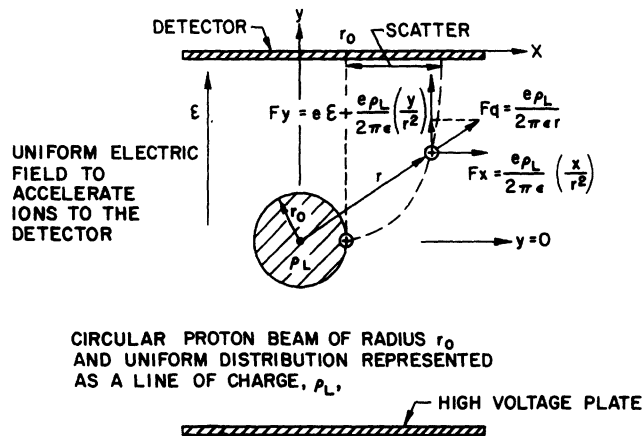


Fig. 3 Model illustrating coulomb force scattering of residual gas ions.

the beam surface. The line of charge is $\rho_L = I_L/v_p$ where v_p is the proton velocity at 50 MeV and I_L is the linac beam current. For a linac beam current of 20 mA with a diameter of 2.5 cm, ρ_L is ≈ 2.2 coulombs/meter and the electric field intensity is 3.2 V/cm at the beam surface. A comparison between calculated and measured values of the ion scattering due to coulomb forces as a function of electrode field strength is shown in Fig. 4. The deviation at low field strengths is attributed to the assumptions of proton beam size and distribution used in the calculations. At an electric field intensity of 260 V/cm, the calculated amount of scatter is less than 1/2 mm for an ion collection path length of 3.8 cm. Thus the effects of coulomb scattering can be minimized utilizing reasonable values of electric field intensities.

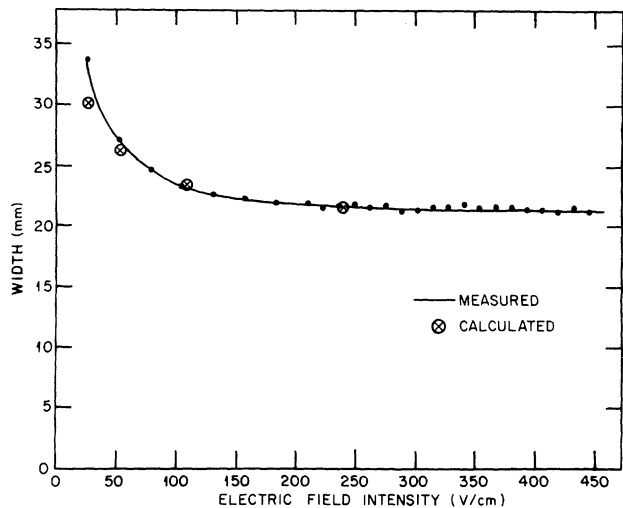


Fig. 4 Comparison of calculated and measured values of ion scatter as a function of electrode field strength.

The collection time to accelerate the ions or electrons to the strip electrode, neglecting coulomb forces and initial energies, is given in Fig. 5. In the 50 MeV beam line system, at a field strength of 260 V/cm and collection path length of 3.8 cm, the ion collection time (using a weighted average mass for air ions) is 0.94 μ s as compared to a collection time of 4.05 ns for electrons. Since the proton beam is approximately 2.5 cm wide, there is a range of collection path lengths which results in a time spread for collecting all the ions produced at a given instant by the proton beam. This collection time spread is 0.3 μ s for ion collection under the above conditions. This time spread limits the use of ion collection for very fast time sampling systems.

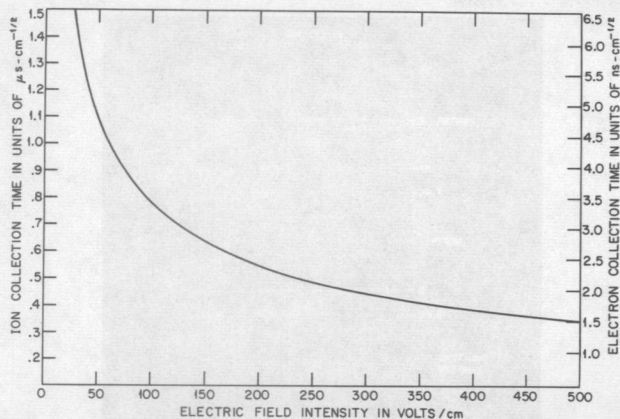


Fig. 5 Ion and electron collection time as a function of electrode field strength.

Utilizing electron collection, observations were made to determine the characteristics of the liberated electrons. Even with no collecting field on the electrode, electrons will strike the strip electrode due to their kinetic energy. Using the secondary screen as a potential barrier, it was found that over 90% of the electrons had an energy, normal to path of the beam, of less than 10 eV. The most probable energy was a few electron volts. This kinetic energy could result in an erroneous detected beam profile. Interestingly, under identical electrode operating conditions, the detected incremental beam profile yields a slightly narrower beam width when using electron collection than that found using ion collection. This suggests that the focusing affect on the liberated electrons by the beam, due to coulomb forces, overcomes the kinetic energy scattering. Investigations are continuing to study this phenomenon.

Electronics and Signal Displays

An analog voltage signal is obtained from each strip on the detection electrode using current-to-voltage converters. Cable drivers are then used to transfer the signals to a data station. In the case of the synchrotron system, the signals are sent to a data station in the Main Control Room.

At the data station, the analog signals have been processed in a variety of ways. Originally, only a sequential multiplexer was used to sample the analog signal from each strip to obtain a single output which, when displayed on an oscilloscope, yields an incremental beam density profile. To provide measurements at selected magnet field values, the multiplexer sequentially sampled the strip signals upon command. Many observations and studies were made using this system, but it was limited in providing

continuous information throughout the acceleration cycle.

To obtain dynamic quantitative information, the strip signals from the radial and vertical electrodes were connected to the ZGS Monitor system.¹⁰ During acceleration, the strip signals were digitized and transferred to the control computer. The computer then calculated the radial and vertical beam size, and the results were plotted on the CRT display unit¹¹ along with the beam intensity as shown in Fig. 6. The display shows the following quantities over the selected 2 kG to 19 kG magnet field period: (1) the 10%, 50%, and 90% locations of the vertical profile integral which is the height containing 80% of the beam, and the beam center of charge; (2) the difference between the 10% and 90% locations of the radial profile integral which is the width of 80% of the beam; and (3) the beam intensity in units of $1(10)^{12}$ protons. This system proved to be an invaluable tool for studying beam behavior throughout the acceleration cycle.

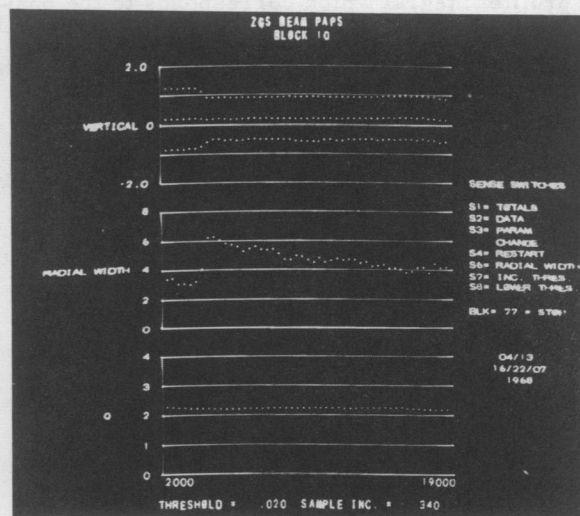


Fig. 6 Computer CRT display of beam size during acceleration.

In early 1968, data was obtained with the 50 MeV beam line monitor. Figure 7 is a block diagram of the system used to acquire the data from the detector. A 1 MHz multiplexer was utilized with appropriate delay in each channel, such that, the output signal corresponds to an instantaneous $1 \mu\text{s}$ sample of the beam density profile. The ZGS Monitor with its high speed data acquisition station was used to digitize and transfer the profile signals to the control computer. The multiplexer profile output was digitized every $10 \mu\text{s}$ for a maximum of 20 profile measurements during the linac beam pulse. The

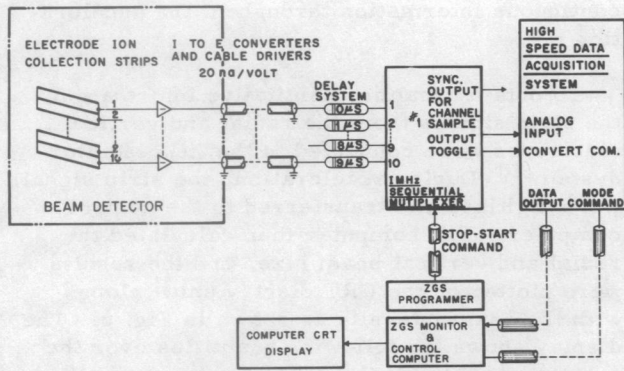


Fig. 7 Block diagram of 50 MeV beam line monitoring system.

computer results were plotted on the CRT display unit as shown in Fig. 8. The computer calculated and plotted the following quantities for each of the 20 beam profiles measured: (1) the relative current which is the integral under each profile histogram which is proportional to the instantaneous linac beam current; (2) the 50% location of the profile integral which corresponds to the position of the center of charge of the beam; and (3) the difference between the 10% and 90% locations of the profile integral which is the width of 80% of the beam. Two linac beam pulses were displayed, one being stored in the display unit as a reference, and the second a pulse to pulse or on-line measurement. In this way, studies could be made of the effects of different linac parameters by comparing measurements after a parameter was changed.

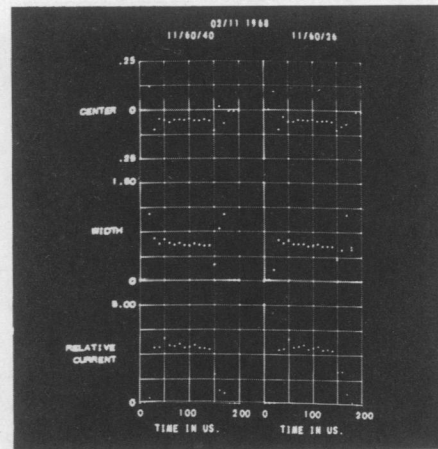


Fig. 8 Computer CRT display of 50 MeV beam parameters.

To assist the machine operators in tuning the ZGS, an analog system was installed which provides calibrated output signals of the accelerated beam radial width and vertical height. A system block diagram is shown in Fig. 9. The sequential multiplexer is used to sample the signal from each strip to obtain the incremental profile. Since each strip is of known size and position in the vacuum chamber, the multiplexer output sampling rate is calibrated in distance. A 1 MHz multiplexer is used to sample the ten electrode strips which are 3.8 cm wide on the radial electrode, thus the output sweep rate is 3.8 cm/ μ s. The profile signal is integrated and compared, using two integrated circuit comparators, to the total ion signal detected. The total ion signal is

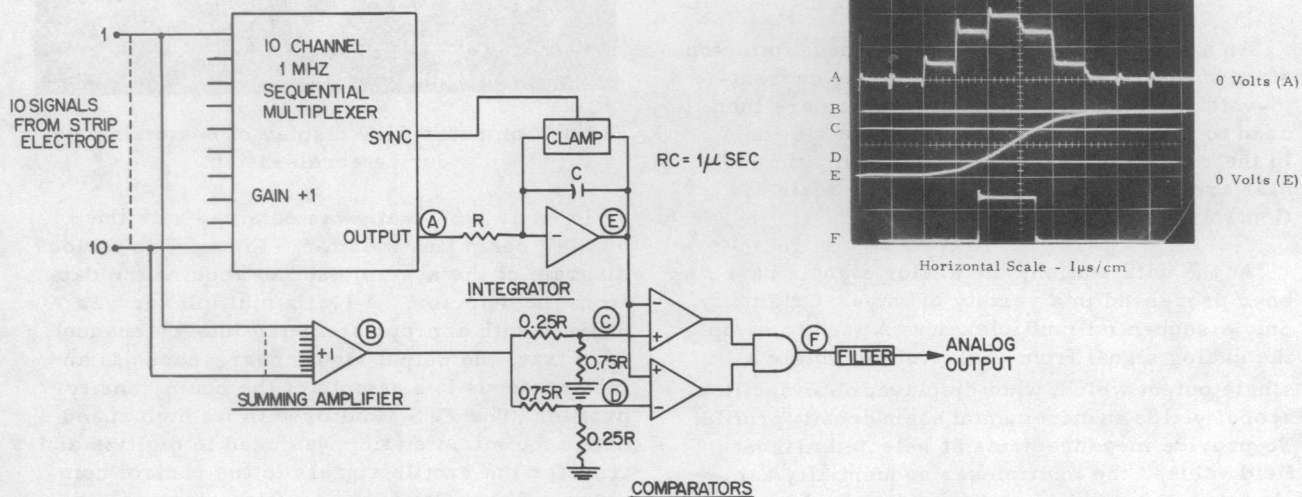


Fig. 9 Block diagram of system used to obtain 50% beam width analog signal.

obtained by summing the inputs to the multiplexer. The output of the two comparators are connected to an AND gate whose output is high only when the integrator signal is within the reference levels on the comparators. The comparator reference levels are set to be some fraction of the ion sum signal which is determined by the beam contour to be found. For example, if the beam width which contains 50% of the protons is to be found, the 25% and 75% levels of the ion sum signal are used as the comparator reference levels. When the integrator signal is larger than 25% of the sum signal, the output of the AND gate goes high and when the integrator output is larger than 75% of the ion sum signal, the gate goes low. The AND gate output signal has the same calibration with respect to vacuum chamber distance as the multiplexer output. Filtering the gate output provides the analog signal for monitoring the beam size. Since the multiplexer cycles every $11 \mu\text{s}$ ($1 \mu\text{s}/\text{channel}$ and $1 \mu\text{s}$ integrator clamp time) the beam size output signal is calibrated in volts per vacuum chamber distance. The AND gate voltage equals eleven strip widths.

Two such systems used in conjunction with the radial and vertical detection electrodes yield the vertical and radial size containing 50% of the beam. A calibration of 1 V/inch is achieved using amplifiers with appropriate gain values. Figure 10 is an oscilloscope display showing the vertical and radial beam size, along with beam intensity and position. This system has been used extensively to observe the effects of various machine parameters on the beam size and damping throughout acceleration.

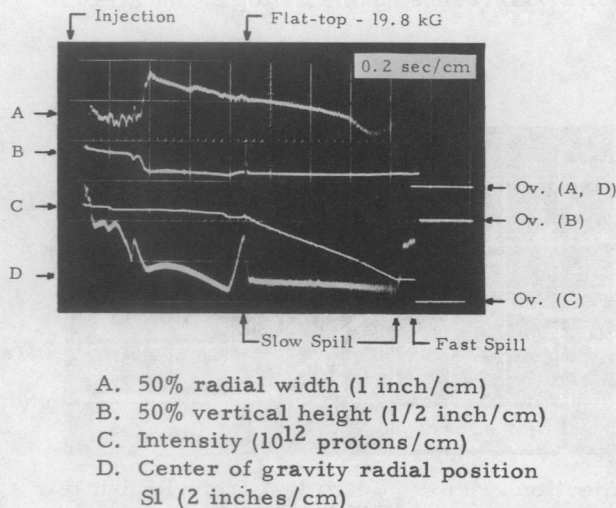


Fig. 10 Analog beam size signals during acceleration.

A diagonally cut rectangle, 76 cm wide and 5.8 cm long (in the direction of the beam travel) was added to the radial strip electrodes in the synchrotron for finding the position of the beam center of charge. The ratio of the difference over the sum of the two ion collection signals yields a measure of beam position. Figure 11 shows the system block diagram, and Fig. 10 the resulting position signal.

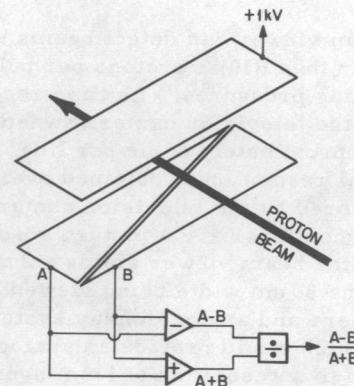


Fig. 11 Block diagram of beam center of charge position system.

Sensitivity and Resolution

As stated previously, a circulating beam current of 300 mA yields a detected ion current of approximately 10.4 nA per centimeter length of collection at a beam energy of 12 GeV. Since the synchrotron radial electrode strips are 5.1 cm long and the ground and secondary screens each allow 75% transmission, the total detected ion current signal is 30 nA. Using amplifiers and drivers with a transconductance of 100 nA/V, a total analog signal of 300 mV is obtained. This signal is divided among the strips according to the width and distribution of the beam under the strips. The present synchrotron system has been used to detect beam intensities from $2(10)^{11}$ to $3(10)^{12}$ by adjustment of amplifier transconductance and vacuum chamber pressure.

The strip electrode detector can be regarded as a parallel input system and thus can provide good time resolution. The 50 MeV beam line system yielded an instantaneous $1 \mu\text{s}$ sample of the beam profile utilizing ion collection. Narrower sample times can be achieved using electron collection, limited only by the bandwidth of the associated electronics.

Spatial resolution, when using an incremental

profile, is determined by the strip to beam size ratio and the analog or digital data processing. To determine the width of 50% of the proton beam to an accuracy of better than 10%, the beam must be at least three strips wide. If the beam is less than three strips wide, the error is a function of beam location with respect to the strips. For instance, a beam one strip wide may be detected as a beam two strips wide if centered between two adjacent strips. This results in a 100% error. Thus the strip width is determined by the expected beam size and accuracy required.

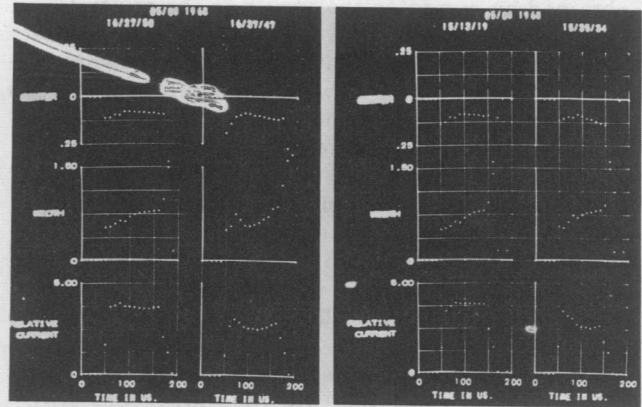
The beam viewer can detect beams with intensities lower than $1(10)^{10}$ protons per pulse at normal operating pressures. Its time resolution is limited by the television camera sweeping rate, which is approximately $60 \mu\text{s}$ per line. However, good spatial resolution is obtained over the entire area monitored by the television camera. Since television monitors have a picture resolution of 400 lines, the beam viewer yields a 2 mm resolution over the 80 cm width being viewed. A television camera and analog display system are planned, which would provide an analog output of beam width to a resolution of 1 mm over the 80 cm width of the ZGS beam aperture. It is hoped that scanning rates of $10 \mu\text{s}$ or less can be achieved.

Results and Observations

Using the 50 MeV proton line system, studies were made to observe the effects on beam position, size, and relative intensity at the detector due to changes in various linac parameters. In Fig. 12, the reference data corresponds to arbitrary conditions during tuneup and the response of the beam to the following conditions can be observed: Fig. 12a, a reduction of the preaccelerator high voltage; Fig. 12b, a reduction of the tank RF level. Both parameters caused changes in the size, position and intensity of the beam emerging from the linac. More monitoring stations are required to fully interpret the beam characteristics, since the parameters adjusted effect the phase space of the emerging 50 MeV beam. Work is continuing in this area.

One of the first observations made with the synchrotron vertical monitoring system was a 1 cm shift of the vertical median plane at injection when the original beam viewer electrode was energized. The median plane shift lowers the vertical aperture bringing about a reduction in accelerated beam intensities. The situation was remedied by modifying the beam viewer electrode to that given in Fig. 2.

Ion detection can also provide position and profile measurements for unbunched beam, that



- a -

- b -

Fig. 12 50 MeV beam response to linac parameter changes: a. reduction in preaccelerator high voltage; b. reduction in tank RF level.

is, beam that is not under RF control. The total ion collection signal is a relative measure of beam intensity. When used in conjunction with the Slow Q induction signal, the ion signal is helpful in optimizing beam targeting. The Ion Sum and Slow Q signals are shown in Fig. 13. The ion signal provides a measure of that beam, during flattop, which was not targeted because it escaped RF control. This beam, since it is unbunched, is lost at the end of flattop. The beam viewer has been used to determine the slope of the magnet field during flattop by observing the change in the position of unbunched beam. A radial position change of 0.6 cm can be measured for a 5 kG change during flattop at the ZGS.

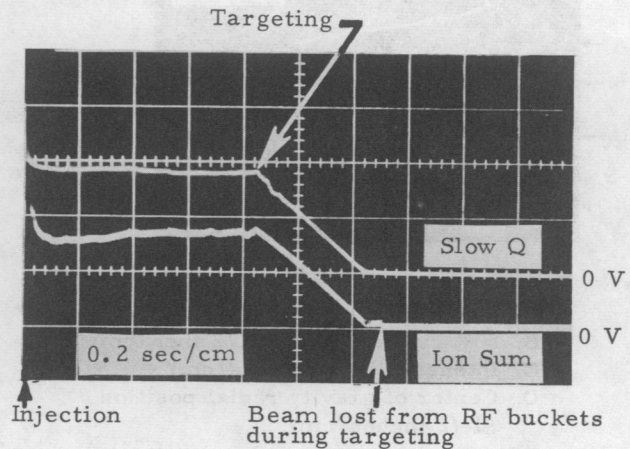


Fig. 13 Comparison of beam intensity and total ion signals.

Early studies with the beam viewer showed a radial growth starting at 8 kG with an intensity threshold of approximately $1(10)^{12}$ protons. Later computer plots showed a radial growth near 4 kG for beam intensities of $2(10)^{12}$ protons, as illustrated earlier in Fig. 6 (the corresponding reduction in vertical height is unexpected and being investigated).

One observation made recently is illustrated in Fig. 14. The ZGS vertical damping system was gated off from 3.5 kG to 5 kG. It can be seen from the photographs that if the radial growth occurred before 3.5 kG, as in Fig. 14a, the beam could be accelerated to full energy without incident. If, however, the radial growth did not take place before the vertical damper was gated off, a vertical blowup would occur immediately upon turnoff, as in Fig. 14b. The beam intensity in both cases was $2.6(10)^{12}$ protons.

A damping system has recently been installed to suppress the radial growth. While testing the system, it was observed, Fig. 15, that at 150 ms after injection (≈ 3.5 kG), a radial blowup occurred. After a beam loss, the system was able to damp the beam to its original size. Increasing the damper drive signal eliminated this blowup.

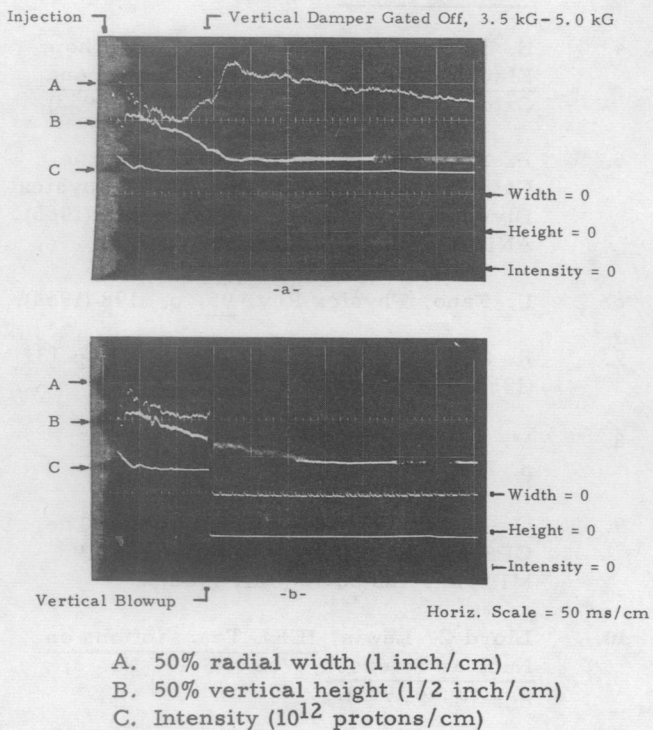


Fig. 14 Dependence of vertical beam stability on radial width: a. with radial growth; b. with no radial growth.

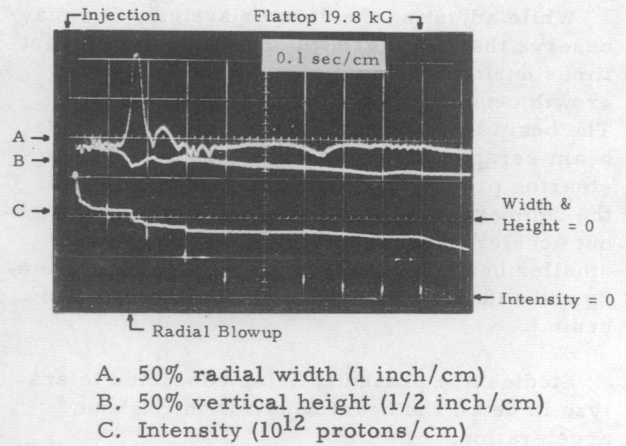


Fig. 15 Radial blowup during acceleration.

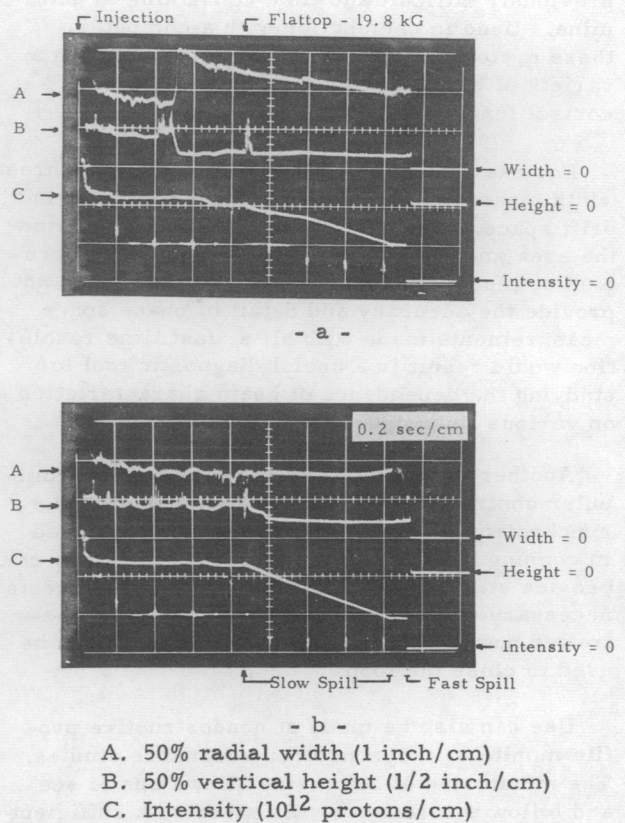


Fig. 16 Damping the radial growth throughout acceleration: a) during tuneup; b) after tuneup.

While adjusting the damper system, one may observe the radial growth occurring at different times during acceleration. In Fig. 16a, the growth occurs 480 ms after injection (≈ 11 kG). The beam loss at 680 ms is caused by the wide beam scraping the inside aperture due to the steering program. However, proper tuning of the damper eliminates the radial growth throughout acceleration as shown in Fig. 16b. The smaller beam size increases extraction efficiency and reduces random structure on extracted beam.

Studies are presently being conducted to analyze in detail the beam behavior throughout acceleration.

Conclusions

Nondestructive beam monitoring is a useful diagnostic tool for assisting in accelerator studies and operations. Present systems provide on-line measurements of parameters which were previously difficult and time consuming to determine. Used in conjunction with a computer, these systems can be expanded to accomplish a variety of beam monitoring, diagnostic, and control functions.

For example, in the 50 MeV proton line, three width measurements taken at three locations in a drift space, provide sufficient data to determine the area and orientation of the phase space occupied by the beam. While such a system does not provide the accuracy and detail of phase space measurements made with slits, fast time resolution would result in a useful diagnostic tool for studying the dependence of beam characteristics on various linac operating parameters.

Another obvious extension is the on-line computer control of matching the linac beam to the synchrotron. Data from profile monitors used in conjunction with a beam transport program can provide steering and quadrupole magnet currents necessary for proper matching. Digitally controlled power supplies on these magnets may be used to close the loop.

Use can also be made of nondestructive profile monitors in synchrotron resonance studies. The monitoring of beam size allows one to see and follow a resonance. By steering a sufficiently low intensity beam on a particular resonance throughout acceleration, a useful machine tune plot can be obtained. Once this is accomplished, a more complete insight can be made into the synchrotron damping mechanism and beam behavior may be studied in detail.

Acknowledgements

The efforts of many people were necessary in the culmination of the many systems. In particular, I would like to thank F. Hornstra, Jr. for his thoughts and many discussions, as well as M. F. Shea for his observations and assistance in the design and installation of the 50 MeV beam line system. Without the close cooperation and assistance of the Central Computer Control Group, the computer analysis and displays would not have been possible. In addition, I would like to thank Dr. F. Rieke for his assistance in determining the theoretical primary ionization by protons in air.

References

1. F. Hornstra, Jr. and W. H. DeLuca, Proceedings of the Sixth International Conference on High Energy Accelerators p. 374 (1967).
2. W. H. DeLuca and M. F. Shea, Proceedings of the 1968 Proton Linear Accelerator Conference Part I, p. 190 (1968).
3. E. W. McDaniel, Collision Phenomena in Ionized Gases, Wiley, New York (1954).
4. H. S. W. Massey and E. H. S. Burhop, Electronic and Ionic Impact Phenomena, Oxford University Press, Oxford (1952).
5. F. Rieke and W. Prepejchal, Argonne National Laboratory Radiological Physics Division Annual Report, ANL-7060 (1965), ANL-7220 (1966), ANL-7360 (1967).
6. U. Fano, Physics Rev. 95, p. 1198 (1954).
7. R. Sternheimer, Physics Rev. 115, p. 137 (1959).
8. M. E. Rudd, et al, Physics Rev. 151, p. 20 (1966).
9. C. D. Johnson and L. Thorndahl, "The CPS Ionization Beam Scanner (IBS)," MPS/Int. CO 68-13 (July 1968).
10. Lloyd G. Lewis, IEEE Transactions on Nuclear Sciences, Vol. NS-12, No. 3, p. 1 (June 1965).
11. Lloyd G. Lewis, 1969 Particle Accelerator Conference, Session H (March 1969).